Binding of ZO-1 to α5β1 integrins regulates the mechanical properties of α5β1–fibronectin links

Víctor González-Tarragó[a,b], Alberto Elosegui-Artola[a], Elsa Bazellières[c], Roger Oria[a,b], Carlos Pérez-González[a,b], and Pere Roca-Cusachs[a,b,*]

[a]Institute for Bioengineering of Catalonia and [b]University of Barcelona, 08028 Barcelona, Spain; [c]IBDM, Institut de Biologie du Développement de Marseille, UMR 7288, 13009 Marseille, France

ABSTRACT **Fundamental processes in cell adhesion, motility, and rigidity adaptation are regulated by integrin-mediated adhesion to the extracellular matrix (ECM). The link between the ECM component fibronectin (fn) and integrin α5β1 forms a complex with ZO-1 in cells at the edge of migrating monolayers, regulating cell migration. However, how this complex affects the α5β1-fn link is unknown. Here we show that the α5β1/ZO-1 complex decreases the resistance to force of α5β1–fn adhesions located at the edge of migrating cell monolayers while also increasing α5β1 recruitment. Consistently with a molecular clutch model of adhesion, this effect of ZO-1 leads to a decrease in the density and intensity of adhesions in cells at the edge of migrating monolayers. Taken together, our results unveil a new mode of integrin regulation through modification of the mechanical properties of integrin–ECM links, which may be harnessed by cells to control adhesion and migration.**

Monitoring Editor
Andres J. Garcia
Georgia Institute of Technology

Received: Jan 11, 2017
Revised: Feb 23, 2017
Accepted: Feb 24, 2017

INTRODUCTION

General processes in development, wound healing, or cancer are driven by cell adhesion and migration, which are determined by the interaction between cells and the extracellular matrix (ECM; An *et al.*, 2009). This interaction is largely mediated by integrins, and specific ECM–integrin links such as those formed by the ECM protein fibronectin (fn) and integrin α5β1 are involved in crucial cellular processes in signaling and mechanotransduction (Katsumi *et al.*, 2004; Elosegui-Artola *et al.*, 2014). Integrin-mediated functions are regulated by a myriad of integrin-binding adaptor proteins (Calderwood, 2004; Roca-Cusachs *et al.*, 2012), which can affect both their activation and biochemical signaling (Ghatak *et al.*, 2013; Hytönen and Wehrle-Haller, 2015) and their mechanical properties (Ciobanasu *et al.*, 2013; Goldmann *et al.*, 2013; Das *et al.*, 2014). In turn, the affinity and mechanical properties of integrin–ECM links (and specifically of α5β1–fn links) regulate mechanotransduction and the ability of cells to both transmit forces to the substrate and transduce them into downstream biochemical signals (Elosegui-Artola *et al.*, 2014, 2016). Thus regulation of integrin mechanics by adaptor protein interactions emerges as a potential way to tune mechanotransduction.

An adaptor protein described to bind to α5β1 is tight junction protein ZO-1, which is generally localized to cell–cell adhesions (Fanning, 1998; González-Mariscal *et al.*, 2008) but binds to the α5 subunit of α5β1 (Taliana *et al.*, 2005; Tuomi *et al.*, 2009). The formation of this complex affects cell motility (Tuomi *et al.*, 2009) and is crucial for cytokinesis (Hämälistö *et al.*, 2013). The formation of the α5β1/ZO-1 complex is mediated by protein kinase Cε–dependent phosphorylation of ZO-1. Once phosphorylated, ZO-1 then translocates to cell lamellipodia, but only in subconfluent cells. This interaction is believed to stabilize and polarize cells because if disrupted, directional persistence and migration velocity are modified in different cell types (Tuomi *et al.*, 2009; Bazellières *et al.*, 2015). Of interest, alterations in α5β1 and ZO-1 are related to malignant phenotypes (Roman *et al.*, 2010; Ni *et al.*, 2013; Paul *et al.*, 2015). Thus ZO-1 acts as a regulator of α5β1 integrins, and we hypothesized that its effect could be mediated by changes in mechanical properties of the α5β1–fn link.

RESULTS AND DISCUSSION

Disruption of the α5β1/ZO-1 complex affects cell motility

In this study, we used the human mammary epithelial cell line MCF10A, the migration of which has been previously studied (Bazellières *et al.*, 2015; Vincent *et al.*, 2015). To check that ZO-1 was

This article was published online ahead of print in MBoC in Press (http://www.molbiolcell.org/cgi/doi/10.1091/mbc.E17-01-0006) on March 1, 2017.

*Address correspondence to: Pere Roca-Cusachs (rocacusachs@ub.edu).

Abbreviations used: Aα5β1, α5β1 blocking antibody; bBSA, biotinylated bovine serum albumin; ECM, extracellular matrix; fn, fibronectin; MLC, myosin light chain 2; pMLC, phosphomyosin light chain 2.

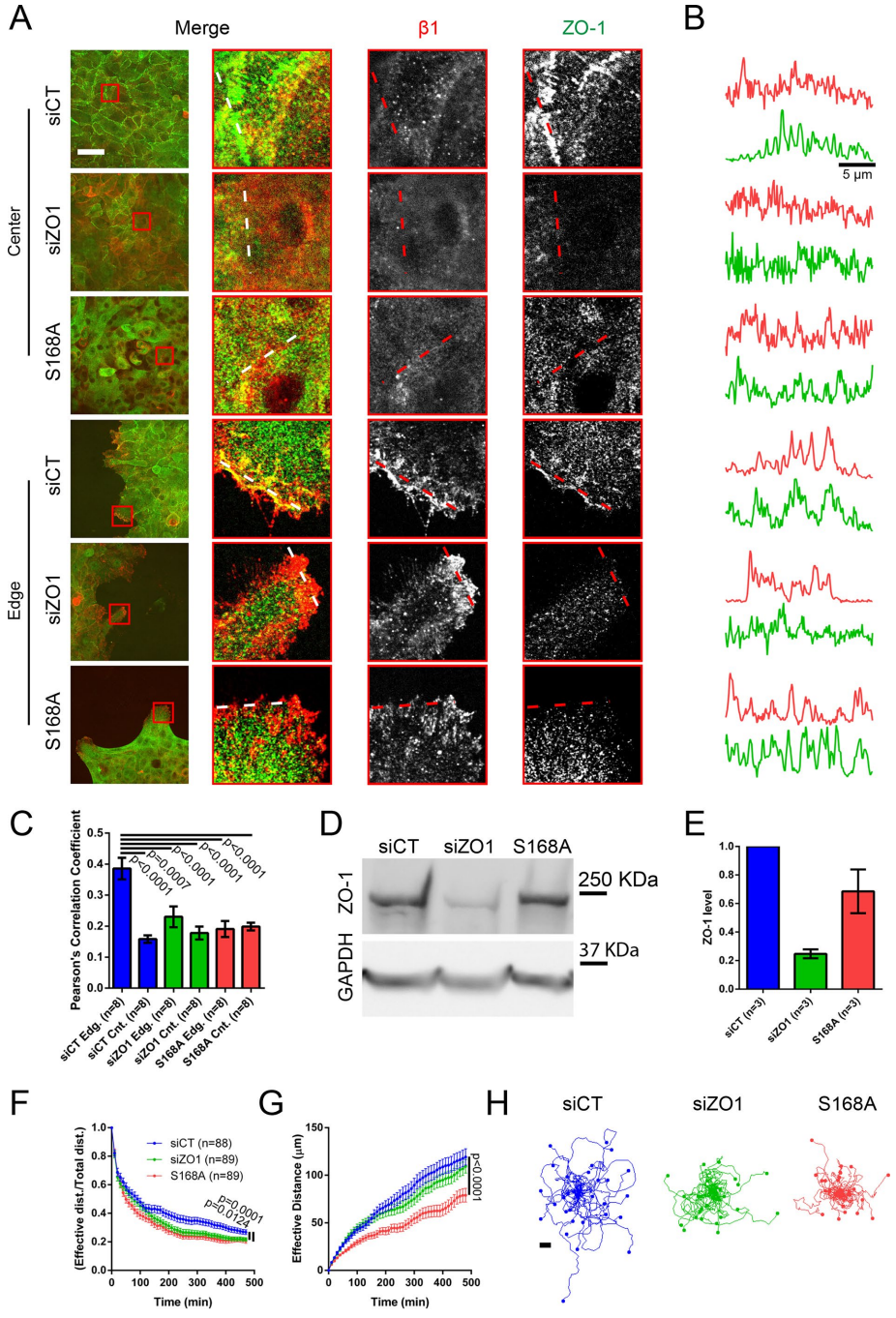

FIGURE 1: ZO-1 forms a complex with α5β1 at the edge of monolayers that affects cell motility. (A) ZO-1 and α5β1 staining of cells at the edge and center of monolayers of cells transfected with nontargeting siRNA (siCT), ZO-1 siRNA (siZO-1), and the ZO-1 plasmid (S168A) seeded on 12-kPa gels coated with fn. FLAG antibody was used to stain for ZO-1 S168A. Insets show the area marked with a red square. Scale bar, 50 μm. (B) Normalized profile plots of the ZO-1 and α5β1 intensity profiles shown in the red lines in A. Scale bar, 5 μm. (C) Pearson's *r* of ZO-1 and α5β1 stainings at the edge and center of monolayers. (D) ZO-1 Western blot of cells transfected with nontargeting siCT, ZO-1 siZO-1, and S168A. (E) Quantification of the Western blot of cells transfected with siCT, siZO-1, and S168A. (F) Directional persistence of migrating single cells (effective distance/total distance) on 12-kPa gels coated with fn. Significant differences were found between siCT and other conditions ($p = 0.0123$ and 0.0001, respectively). (G) Effective distance of migrating single cells on 12-kPa gels coated with fn. Significant differences were found between S168A and other conditions ($p < 0.0001$). (H) Migrating single-cell tracks (480 min) for each condition ($n = 30$). Error bars represent the SEM of *n* number of data points. Images are representative from three experiments.

translocating to the lamellipodia of cells at the edge of monolayers, we seeded a monolayer of cells on 12-kPa gels coated with 10 μg/ml of fn and stained them for activated β1 and ZO-1. As previously described (Tuomi *et al.*, 2009), ZO-1 localized to cell–cell contacts in confluent cells and to the lamellipodia in cells at monolayer edges (Figure 1, A and B), that is, cells with a free edge without cell–cell contacts. Accordingly, colocalization with α5β1 was significantly increased only at lamellipodia (Figure 1C).

To study the effects of the α5β1/ZO-1 complex, we impaired its formation by using a combination of small interfering RNA targeting ZO-1 (siZO1) and independently by transfecting a dominant-negative ZO-1 plasmid (S168A) that impairs binding of endogenous ZO-1 to α5 (Tuomi *et al.*, 2009; Hämälistö *et al.*, 2013). As a control, we used cells transfected with a nontargeting siRNA (siCT). ZO-1 concentrations decreased to ~25% in siZO1 and were only slightly affected in S168A-transfected cells (Figure 1, D and E). Whereas it still localized to cell–cell junctions, ZO-1 had reduced expression in siZO1 cells both at the center and at the edge of monolayers (Figure 1A). Consistent with its reported inability to bind α5, S168A did not localize to lamellipodia or colocalize with α5β1 in any case (Figure 1, A–C). Confirming the dominant-negative effect of S168A, total ZO-1 in S168A cells was also unable to localize to lamellipodia, whereas it localized normally, as expected, to cell–cell junctions (Supplemental Figure S1).

Previous studies demonstrated a role of the α5β1/ZO-1 complex in cell migration in different cancer cell lines (Tuomi *et al.*, 2009). To verify this in our system, we seeded cells on the same 12-kPa gels. We then tracked the cells for 8 h and assessed their directional persistence as the ratio between their effective traveled distance (radial distance from the starting point) and their total traveled distance (sum of the total path). As previously shown, siZO1 and S168A cells were significantly less directional than siCT (Figure 1, F–H).

Thus, in agreement of previous work (Tuomi *et al.*, 2009), our data confirmed that ZO-1 localizes to the lamellipodia of monolayer edge cells, and depleting ZO-1 or preventing its association with α5 affects cell migration.

ZO-1 binding to α5 decreases integrin–fn adhesion resistance to force

To investigate whether ZO-1 binding to α5β1 affected the α5β1–fn link, we used a previously described setup based on

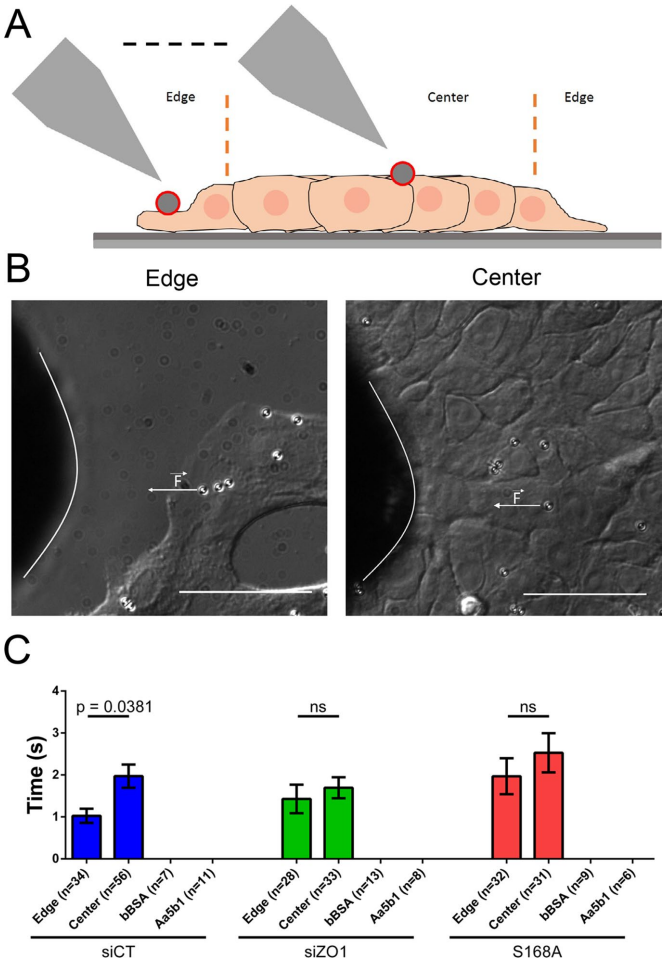

FIGURE 2: Disruption of the α5β1/ZO-1 complex increases α5β1–fn link resistance to forces only at the edge of monolayers. (A) Cartoon depicting the experimental setup with magnetic tip pulling on beads attached to cells both at the edge and center of cell monolayers. (B) Magnetic tip applying a magnetic field producing 0.5 nN of force to beads both at the edge (left) and at the center (right) of monolayers. (C) Time taken to detach beads for each condition either at the center or at the edge of monolayers. Beads were coated with FN7-10 (with or without incubating with Aα5β1) or bBSA. No significant differences were found between centers ($p = 0.7887$) among conditions. Scale bar, 50 μm. Images are representative from four experiments.

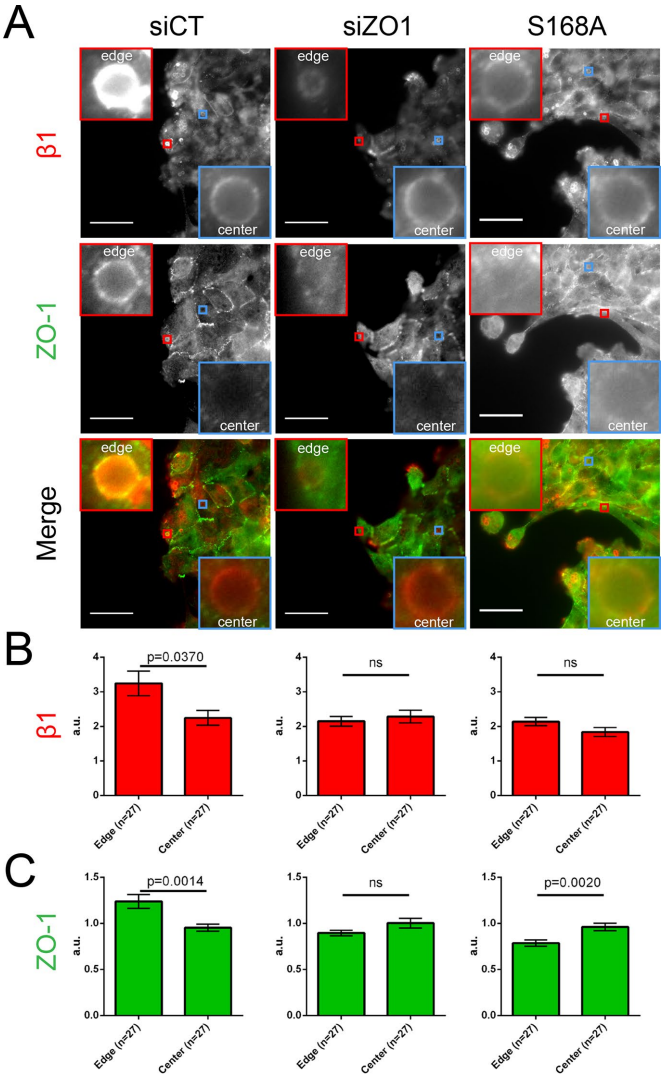

FIGURE 3: Disruption of the α5β1/ZO-1 complex decreases α5β1–fn recruitment at the edge of monolayers. (A) β1 and ZO-1 staining of silica beads coated with FN7-10 attached to monolayers. (B) β1 recruitment to silica beads coated with FN7-10 attached at the edge and at the center of monolayers. (C) ZO-1 recruitment to silica beads coated with FN7-10 attached at the edge and at the center of monolayers. FLAG antibody was used to stain for ZO-1 S168A. Scale bar, 50 μm. Insets show the area marked with red/blue squares. Images are representative from three experiments.

magnetic tweezers (Elosegui-Artola *et al.*, 2014). We first coated superparamagnetic beads with FN7-10, a fn fragment (Coussen *et al.*, 2002; Elosegui-Artola *et al.*, 2014) that binds mechanically to cells primarily through α5β1 (Roca-Cusachs *et al.*, 2009). We allowed beads to attach to cell monolayers for 35 min and then pulled on them using the magnetic tweezers with a force of 0.5 nN until beads detached both at the subconfluent edge and at the center of monolayers within the same sample (Figure 2, A and B).

In siCT cells, bead detachment times significantly decreased at monolayer edges with respect to the monolayer center (Figure 2C). This difference was lost both in siZO1 cells and in cells transfected with S168A, showing that this differential regulation is mediated by ZO-1 and its ability to bind α5. As negative controls, beads detached immediately when coated with either biotinylated bovine serum albumin (bBSA) or FN7-10 in cells preincubated with an α5β1 blocking antibody (Aα5β1) (Figure 2C). This indicates that the measured adhesion strength was specific to fn and mediated by α5β1 integrins. We note that despite certain sample-to-sample variability, we did not observe significant differences between conditions at monolayer centers, further suggesting that ZO-1 had a differential effect on monolayer edges.

Formation of the α5β1/ZO-1 complex increases α5β1–fn recruitment

The measured effects in adhesive strength could be mediated by changes in the resistance to force of integrin–fn links or by changes in integrin recruitment. To assess potential changes in integrin recruitment, we incubated nonfluorescent, FN7-10–coated silica beads with cells (Elosegui-Artola *et al.*, 2014), fixed the cells, and stained them for ZO-1 and activated β1 (Figure 3A) and total β1 (Supplemental Figure S2). All conditions showed recruitment of

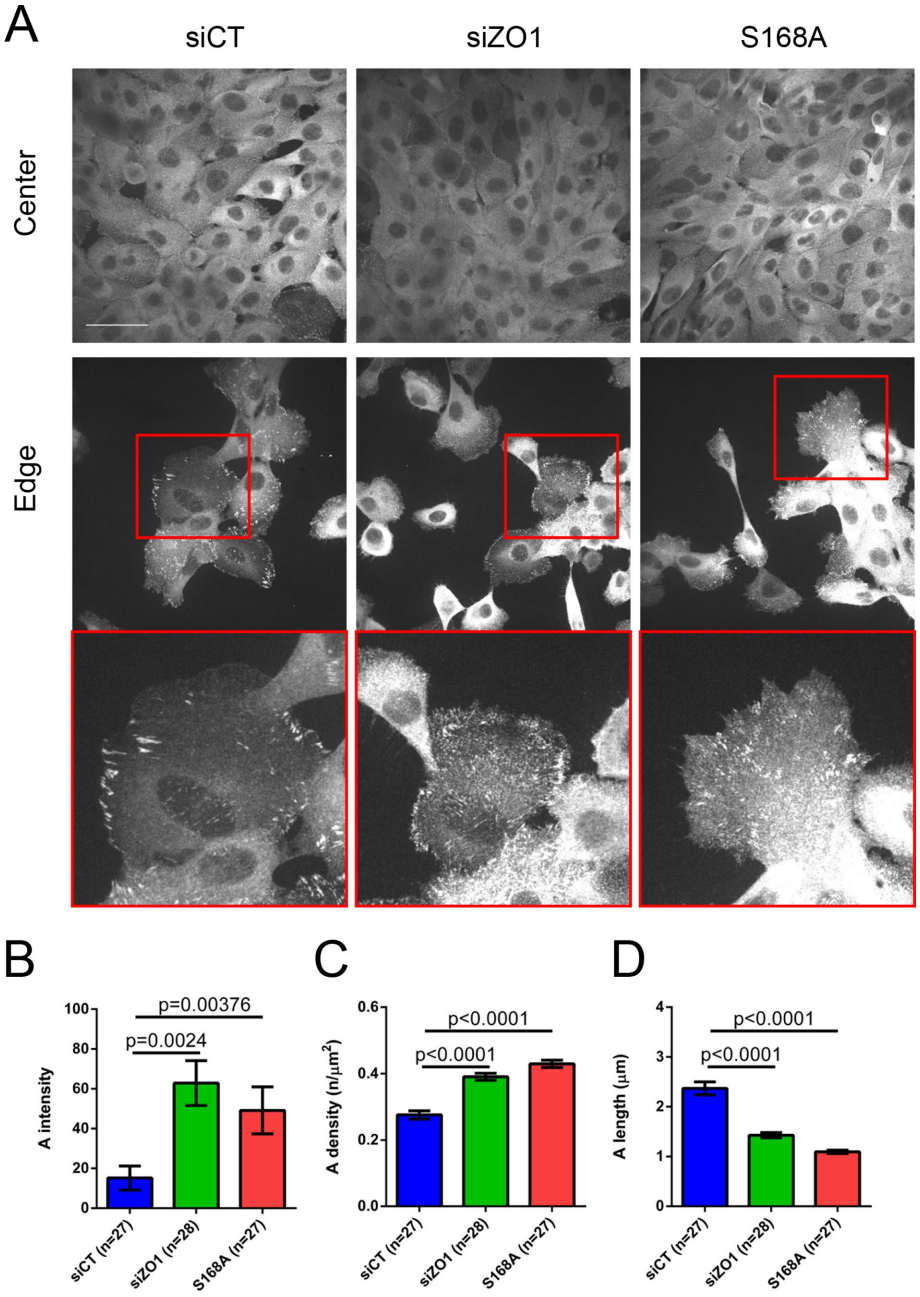

FIGURE 4: Disruption of the α5β1/ZO-1 complex leads to a higher number of smaller nascent adhesions. (A) Paxillin staining at the subconfluent edge and at the center of monolayers. (B) Quantification of adhesion intensity. (C) Quantification of adhesion density. (D) Quantification of adhesion length. Scale bar, 50 μm. Insets show the area marked with a red square. Images are representative from three experiments.

activated and total β1 to beads (Figure 3B and Supplemental Figure S2) both at the edge and at the center of monolayers. Further, beads at the edge of siCT cells increased recruitment of ZO-1 and active (but not total) β1 with respect to the center (Figure 3B and Supplemental Figure S2). Thus, whereas the interaction between ZO-1 and α5β1 occurring specifically at monolayer edges does not affect total integrin population, it increases the recruitment of the active fn-bound α5β1 integrins.

In summary, the interaction between ZO-1 and α5β1 specific to monolayer edges affected α5β1-fn links by increasing their recruitment but reducing their resistance to force. This suggests that cell–bead detachment under force is regulated by the mechanical properties of the links and not by their recruitment (or affinity), which would lead to the opposite result. Further confirming this direct link to the properties of integrin–fn links, neither bead detachment times nor integrin recruitment were affected by impairing cell contractility with blebbistatin (Supplemental Figure S3). Thus our results are consistent with ZO-1 affecting α5β1-fn links specifically at monolayer edges by increasing both their off-rates (i.e., reducing their lifetime under force) and their on-rates (thereby increasing recruitment).

Adhesion formation is affected by the α5β1/ZO-1 complex

According to our previously described molecular clutch model of adhesion formation (Elosegui-Artola *et al.*, 2014), a concomitant increase in both on- and off-rates (likely induced by ZO-1) should decrease force loading in integrins, impairing mechanotransduction, subsequent force transmission, and formation of adhesions. Surprisingly, we did not observe changes in force transmission in the different conditions (Supplemental Figure S4), possibly because the potential decrease mediated by ZO-1 was compensated by increased levels of total and phosphorylated myosin in siCT cells compared with other conditions (Supplemental Figure S3). However, and consistent with model predictions, the number and intensity of paxillin-rich adhesions at monolayer edges decreased in siCT cells compared with siZO-1 cells and cells transfected with S168A (Figure 4, A and B). As expected, we did not observe differences in adhesion formation at the center of monolayers (Figure 4A). Of interest, even though their intensity and density were lower (Figure 4, B and C), adhesions in siCT cells were significantly longer than in other conditions (Figure 4D). This suggests that mechanical regulation of the α5β1-fn link by ZO-1 may readily explain adhesion formation but not later maturation processes, which may depend on other factors (Choi *et al.*, 2008).

Taken together, our results reveal how tight junction protein ZO-1, an integrin regulator, affects the mechanics and dynamics of α5β1–fn adhesions, increasing their affinity and decreasing their ability to withstand forces. Although a detailed confirmation would require a complex in vitro analysis with isolated purified proteins, this effect suggests an increase in both binding and unbinding rates between fn and α5β1. This could explain the associated decrease in adhesion density and intensity caused by ZO-1 at monolayer edges. In turn, the faster binding dynamics caused by ZO-1 association may facilitate the migration of control versus ZO-1–depleted cells by facilitating adhesion remodeling. How ZO-1 association leads to the observed mechanical changes in

α5β1–fn links and the combination of mechanical and biochemical factors by which it affects behaviors such as cell migration remain to be elucidated. Further, those effects may depend on cell type and substrate coating and stiffness, which are affected, for instance, in cancer (Paszek *et al.*, 2005; Plodinec *et al.*, 2012). Whereas we found that ZO-1 depletion decreased myosin phosphorylation and did not affect cell–matrix force transmission, studies using other cell types, matrix coatings, and conditions found even (Fanning *et al.*, 2012) or increased myosin phosphorylation (Tornavaca *et al.*, 2015) and increased contractility (Bazellières *et al.*, 2015; Choi *et al.*, 2016). However, and in general terms, our results exemplify how adaptor proteins can regulate integrin function by affecting not only their activation or affinity for ECM ligands but also their mechanical properties under force.

Previous work showed how adaptor proteins such as talin, α-actinin, or vinculin mediate integrin activation and mechanotransduction, leading to increased adhesion strength and reinforcement (Mierke *et al.*, 2008; Roca-Cusachs *et al.*, 2009). Here we demonstrate an alternative and counterintuitive mechanism by which another adaptor protein (ZO-1) promotes activation but decreases mechanical resistance. Because such mechanical regulation is bound to affect downstream mechanosensing processes, this provides an interesting and novel way to regulate cell adhesion, mechanoresponse, and function in general.

MATERIALS AND METHODS

MCF10A cell culture and transfection

MCF10A cells were grown as described previously (Bazellières *et al.*, 2015) and tested negative for mycoplasma contamination. Cells were transfected using the Lipofectamine 3000 transfection kit (Invitrogen) following manufacturer's instructions using either a pool of three siRNAs (Bazellières *et al.*, 2015) or 5 ng of the plasmid (ZO-1-168S→A-FLAG; S168A), a kind gift from the laboratory of Johanna Ivaska (University of Turku, Finland; Tuomi *et al.*, 2009). Five days after transfection, cells were trypsinized and used for experiments. S168A plasmid has a point mutation in serine 168 that impairs its binding to α5 and is tagged with the FLAG peptide for identification.

Magnetic tweezers and bead-recruitment experiments

Magnetic tweezers experiments were carried out as previously described (Roca-Cusachs *et al.*, 2009; Elosegui-Artola *et al.*, 2014; Bazellières *et al.*, 2015). Briefly, carboxylated 3-µm magnetic beads (Invitrogen) were coated with a mixture of biotinylated pentameric FN7-10 (a four-domain segment of fibronectin responsible for cell binding and containing the RGD and PHSRN motifs; Coussen *et al.*, 2002) and biotinylated BSA at 1:200. For measurements, cells were first plated on silanized coverslips coated with 40 µg/ml laminin (Sigma-Aldrich) to ensure that the α5β1 blocking antibody used to disrupt adhesion to fn affected only cell–bead and not cell–substrate interactions. Fn-coated beads were then deposited on the coverslips for 35 min and attached to cells. The magnetic tweezers were then used to apply a square force of 0.5 nN on beads attached to cells. Cells were imaged using a Nikon Eclipse Ti microscope with a 40× air objective (NA 0.60). The time taken for the beads to detach was assessed.

Immunostaining

Immunostainings on glass and gels were performed as described previously (Elosegui-Artola *et al.*, 2014; Bazellières *et al.*, 2015). Fluorescence images were then acquired with a 60× objective. Adhesion intensity was determined by assessing the mean paxillin intensity on a whole cell normalized to the mean intensity of the cell cytoplasm background. Adhesion density was determined manually by assessing the number of adhesions in an 11-µm^2 circle divided by the area. Adhesion length was measured manually by tracing a line on top of it. To quantify integrin recruitment to beads, FN7-10–coated, 3-µm carboxylated silica beads (Kisker Biotech) were attached to cells, and protein recruitment (with respect to cytoplasmic levels) was calculated assessing the fluorescence intensity of beads (I_{bead}), the cytoplasm ($I_{cytoplasm}$), and image background ($I_{background}$) as

$$\text{a.u.} = \frac{I_{bead} - I_{background}}{I_{cytoplasm} - I_{background}} \quad (1)$$

Correlation between ZO-1 and β1 intensity images was measured by calculating Pearson's *r* by using ImageJ plug-in JACoP (Bolte and Cordelières, 2006).

Preparation of polyacrylamide gels and traction measurements

Polyacrylamide gels of 12 kPa were prepared as described by Kandow *et al.* (2007) and incubated with 10 µg/ml fn (Sigma-Aldrich) overnight at 4°C. Gels were then sterilized with ultraviolet light and washed once with phosphate-buffered saline 1× for immediate use. Traction forces were computed using Fourier transform traction microscopy with finite gel thickness (Trepat *et al.*, 2009) as previously described (Serra-Picamal *et al.*, 2012). To calculate cell tractions in cell monolayers, we used a previously described system of polydimethylsiloxane stencils (Bazellières *et al.*, 2015) to pattern cell monolayers on rectangle-shaped monolayers. We then allowed cells to spread for 4 h and calculated tractions as previously described (Bazellières *et al.*, 2015).

Protein quantification

Protein expression levels were measured using Western blot as previously described (Elosegui-Artola *et al.*, 2014; Bazellières *et al.*, 2015). For the quantification of phosphomyosin light chain 2 (pMLC) and myosin light chain 2 (MLC), the membrane was first probed for pMLC, stripped using Restore Western Blot Stripping Buffer (Thermo Fisher Scientific), and then reblocked and reprobed for MLC. Protein concentrations are reported normalized to glyceraldehyde-3-phosphate dehydrogenase (GAPDH) and relative to the control.

Antibodies

Primary antibodies used were anti–ZO-1 rabbit polyclonal (61-7300; Invitrogen), anti-GAPDH mouse monoclonal (6C5; sc-32233; Santa Cruz Biotechnology), anti–myosin light chain rabbit polyclonal (3672; Cell Signaling), anti–phosphomyosin light chain rabbit polyclonal (3671; Cell Signaling), anti-FLAG rabbit polyclonal (F7425; Sigma-Aldrich), anti–activated β1 mouse monoclonal (12G10; ab30394; Abcam), anti-β1 mouse monoclonal (K20; IOTest CD29-FITC; Beckman Coulter), and anti-paxillin rabbit monoclonal (Y113; ab32084; Abcam) at 1:200 for immunostainings and 1:500 for Western blot. For Western blot, the secondary antibodies used were peroxidase-conjugated anti-mouse immunoglobulin G (IgG; 715-035-151; Jackson ImmunoResearch) and peroxidase-conjugated anti-rabbit IgG (Merck Millipore, AP132P) diluted 1:5000. For immunofluorescence, the secondary antibodies used were Alexa Fluor 488 anti-rabbit (A-21206; Invitrogen) and Alexa Fluor 555 anti-mouse (A-21422; Invitrogen) diluted 1:200. To block α5β1 integrin function, the antibody used was anti-α5β1 mouse monoclonal (10 µg/ml; JCS5; MAB1969; Millipore).

Statistical analysis

All independent datasets were first checked for normality using the d'Agostino–Pearson K2 normality test. One-way or two-way (for time-lapse experiments) analysis of variance was performed for more than two comparisons. For one-to-one comparisons, we used a two-sided *t* test. For multiple comparisons, we used a Dunnett modified *t* test. If data sets were not normal, we used a Kruskal–Wallis test. All error bars shown are SEM.

ACKNOWLEDGMENTS

We thank all of the members of P.R-C.'s laboratory and X. Trepat, J. Alcaraz, D. Navajas, and J. Ivaska for technical assistance and discussions. We thank A. Lahiguera-Belenguer, C. Ureña, N. Castro, A. Kosmalska, M. Uroz, P. Jiménez, A. Labernadie, R. Sunyer, V. Conte, and D. Zalvidea for discussions. This work was supported by the Spanish Ministry for Economy and Competitiveness (BFU2016-79916-P and BFU2014-52586-REDT), a Career Integration Grant within the Seventh European Community Framework Programme (PCIG10-GA-2011-303848), the European Commission (Grant Agreement SEP-210342844), the Generalitat de Catalunya Fundació "La Caixa," and Fundació la Marató de TV3 (project 20133330). V.G.-T., A.E.-A., R.O., and C.P.-G. were supported respectively by a Severo Ochoa Grant (Spanish Ministry of Economy and Competitiveness), a Juan de la Cierva Fellowship (Spanish Ministry of Economy and Competitiveness), a FI fellowship (Generalitat de Catalunya), and the Fundació "La Caixa."

REFERENCES

An SS, Kim J, Ahn K, Trepat X, Drake KJ, Kumar S, Ling G, Purington C, Rangasamy T, Kensler TW, *et al*. (2009). Cell stiffness, contractile stress and the role of extracellular matrix. Biochem Biophys Res Commun 382, 697–703.

Bazellières E, Conte V, Elosegui-Artola A, Serra-Picamal X, Bintanel-Morcillo M, Roca-Cusachs P, Muñoz JJ, Sales-Pardo M, Guimerà R, Trepat X (2015). Control of cell-cell forces and collective cell dynamics by the intercellular adhesome. Nat Cell Biol 17, 409–420.

Bolte S, Cordelières FP (2006). A guided tour into subcellular colocalization analysis in light microscopy. J Microsc 224, 213–232.

Calderwood DA (2004). Integrin activation. J Cell Sci 117, 657–666.

Choi CK, Vicente-Manzanares M, Zareno J, Whitmore LA, Mogilner A, Horwitz AR (2008). Actin and alpha-actinin orchestrate the assembly and maturation of nascent adhesions in a myosin II motor-independent manner. Nat Cell Biol 10, 1039–1050.

Choi W, Acharya BR, Peyret G, Fardin M-A, Mège R-M, Ladoux B, Yap AS, Fanning AS, Peifer M (2016). Remodeling the zonula adherens in response to tension and the role of afadin in this response. J Cell Biol 213, 243–260.

Ciobanasu C, Faivre B, Le Clainche C (2013). Integrating actin dynamics, mechanotransduction and integrin activation: the multiple functions of actin binding proteins in focal adhesions. Eur J Cell Biol 92, 339–348.

Coussen F, Choquet D, Sheetz MP, Erickson HP (2002). Trimers of the fibronectin cell adhesion domain localize to actin filament bundles and undergo rearward translocation. J Cell Sci 115, 2581–2590.

Das M, Subbayya Ithychanda S, Qin J, Plow EF (2014). Mechanisms of talin-dependent integrin signaling and crosstalk. Biochim Biophys Acta 1838, 579–588.

Elosegui-Artola A, Bazellières E, Allen MD, Andreu I, Oria R, Sunyer R, Gomm JJ, Marshall JF, Jones JL, Trepat X, *et al*. (2014). Rigidity sensing and adaptation through regulation of integrin types. Nat Mater 13, 631–637.

Elosegui-Artola A, Oria R, Chen Y, Kosmalska A, Pérez-González C, Castro N, Zhu C, Trepat X, Roca-Cusachs P (2016). Mechanical regulation of a molecular clutch defines force transmission and transduction in response to matrix rigidity. Nat Cell Biol 18, 540–548.

Fanning AS (1998). The tight junction protein ZO-1 establishes a link between the transmembrane protein occludin and the actin cytoskeleton. J Biol Chem 273, 29745–29753.

Fanning AS, Van Itallie CM, Anderson JM (2012). Zonula occludens-1 and -2 regulate apical cell structure and the zonula adherens cytoskeleton in polarized epithelia. Mol Biol Cell 23, 577–590.

Ghatak S, Morgner J, Wickström SA (2013). ILK: a pseudokinase with a unique function in the integrin-actin linkage. Biochem Soc Trans 41, 995–1001.

Goldmann WH, Auernheimer V, Thievessen I, Fabry B (2013). Vinculin, cell mechanics and tumour cell invasion. Cell Biol Int 37, 397–405.

González-Mariscal L, Tapia R, Chamorro D (2008). Crosstalk of tight junction components with signaling pathways. Biochim Biophys Acta 1778, 729–756.

Hämälistö S, Pouwels J, de Franceschi N, Saari M, Ivarsson Y, Zimmermann P, Brech A, Stenmark H, Ivaska J (2013). A ZO-1/α5β1-integrin complex regulates cytokinesis downstream of PKCε in NCI-H460 cells plated on fibronectin. PLoS One 8, e70696.

Hytönen VP, Wehrle-Haller B (2015). Mechanosensing in cell-matrix adhesions—converting tension into chemical signals. Exp Cell Res 343, 35–41.

Kandow CE, Georges PC, Janmey PA, Beningo KA (2007). Polyacrylamide hydrogels for cell mechanics: steps toward optimization and alternative uses. Methods Cell Biol 83, 29–46.

Katsumi A, Orr AW, Tzima E, Schwartz MA (2004). Integrins in mechanotransduction. J Biol Chem 279, 12001–12004.

Mierke CT, Kollmannsberger P, Zitterbart DP, Smith J, Fabry B, Goldmann WH (2008). Mechano-coupling and regulation of contractility by the vinculin tail domain. Biophys J 94, 661–670.

Ni S, Xu L, Huang J, Feng J, Zhu H, Wang G, Wang X (2013). Increased ZO-1 expression predicts valuable prognosis in non-small cell lung cancer. Int J Clin Exp Pathol 6, 2887–2895.

Paszek MJ, Zahir N, Johnson KR, Lakins JN, Rozenberg GI, Gefen A, Reinhart-King CA, Margulies SS, Dembo M, Boettiger D, *et al*. (2005). Tensional homeostasis and the malignant phenotype. Cancer Cell 8, 241–254.

Paul A, Danley M, Saha B, Tawfik O, Paul S (2015). PKCζ promotes breast cancer invasion by regulating expression of E-cadherin and Zonula Occludens-1 (ZO-1) via NFκB-p65. Sci Rep 5, 12520.

Plodinec M, Loparic M, Monnier CA, Obermann EC, Zanetti-Dallenbach R, Oertle P, Hyotyla JT, Aebi U, Bentires-Alj M, Lim RY, *et al*. (2012). The nanomechanical signature of breast cancer. Nat Nanotechnol 7, 757–765.

Roca-Cusachs P, Gauthier N, Del Rio A, Sheetz M (2009). Clustering of alpha(5)beta(1) integrins determines adhesion strength whereas alpha(v)beta(3) and talin enable mechanotransduction. Proc Natl Acad Sci USA 106, 16245–16250.

Roca-Cusachs P, Iskratsch T, Sheetz MP (2012). Finding the weakest link: exploring integrin-mediated mechanical molecular pathways. J Cell Sci 125, 3025–3038.

Roman J, Ritzenthaler JD, Roser-Page S, Sun X, Han S (2010). alpha5beta1-integrin expression is essential for tumor progression in experimental lung cancer. Am J Respir Cell Mol Biol 43, 684–691.

Serra-Picamal X, Conte V, Vincent R, Anon E, Tambe DT, Bazellieres E, Butler JP, Fredberg JJ, Trepat X (2012). Mechanical waves during tissue expansion. Nat Phys 8, 628–634.

Taliana L, Benezra M, Greenberg RS, Masur SK, Bernstein AM (2005). ZO-1: lamellipodial localization in a corneal fibroblast wound model. Invest. Ophthalmol Vis Sci 46, 96–103.

Tornavaca O, Chia M, Dufton N, Almagro LO, Conway DE, Randi AM, Schwartz MA, Matter K, Balda MS (2015). ZO-1 controls endothelial adherens junctions, cell-cell tension, angiogenesis, and barrier formation. J Cell Biol 208, 821–838.

Trepat X, Wasserman MR, Angelini TE, Millet E, Weitz DA, Butler JP, Fredberg JJ (2009). Physical forces during collective cell migration. Nat Phys 5, 426–430.

Tuomi S, Mai A, Nevo J, Laine JO, Vilkki V, Ohman TJ, Gahmberg CG, Parker PJ, Ivaska J (2009). PKCepsilon regulation of an alpha5 integrin-ZO-1 complex controls lamellae formation in migrating cancer cells. Sci Signal 2, ra32.

Vincent R, Bazellières E, Pérez-González C, Uroz M, Serra-Picamal X, Trepat X (2015). Active tensile modulus of an epithelial monolayer. Phys Rev Lett 115, 248103.